SINGLE-WALL CARBON NANOTUBE THIN FILMS: PROCESSING MEASUREMENT AND METHODOLOGY

A Thesis
Submitted to the Graduate Faculty
of the
North Dakota State University
of Agriculture and Applied Science

By

Alex John Brown Waters

In Partial Fulfillment of the Requirements
for the Degree of
MASTER OF SCIENCE

Major Department:
Physics

April 2016

Fargo, North Dakota

North Dakota State University
Graduate School

Title

SINGLE-WALL CARBON NANOTUBE THIN FILMS: PROCESSING MEASUREMENT AND METHODOLOGY

By

Alex John Brown Waters

The Supervisory Committee certifies that this ***disquisition*** complies with North Dakota State University's regulations and meets the accepted standards for the degree of

MASTER OF SCIENCE

SUPERVISORY COMMITTEE:

Erik Hobbie
Chair

Alan Denton

Warren Christensen

Sean Burt

Approved:

April 12, 2016
Date

Sylvio May
Department Chair

ABSTRACT

As society advances to desire smaller, faster, and cheaper electronics along with stronger materials, the search for novel materials continues. Thin films made from single wall carbon nanotubes (SWCNTs) offer a possible solution to many of the challenges that materials scientists currently face. Here, a methodology for studying the deformation of thin SWCNT films is investigated during their processing for use in applications such as photovoltaic devices. A variety of methods for manipulating and visualizing these thin films are discussed, along with the setbacks encountered along the path to improving process characterization.

ACKNOWLEDGEMENTS

This thesis and the research that accompanied it could not have been completed without the selfless aid of Dr. Erik Hobbie. He has been a patient teacher, supportive advisor, and encouraging resource. His own excellence in the field consistently inspired me to work harder and delve deeper into the research. His expertise and suggestions were always an email away, and he was quick to respond. As I entered the University, department, and group after seven years of being out of the field, I had a lot of catching up to do in order to excel in classes and research. I appreciate his support, encouragement, and confidence more than he will ever know.

My introduction to research at NDSU was piloted by Dr. John Harris, whose clout throughout the university allowed me to tag along into clean rooms and chemistry labs while I learned about research methods, the importance of failure, and novel ways to succeed in spite of myriad environmental intrusions. John taught me that real research can include many hours working with glue, popsicle sticks, and paint as well as microscopy and spin coating. While I had the honor of presiding at his wedding to his bride, Nicole, I remain forever in his debt.

Abu Taufique became my research partner near the end of my involvement with this project, and his expertise in programming and computer modeling allowed my bench-top work to be realized into quantifiable results. Sam Brown's extensive knowledge of the chemistry side of materials science was invaluable as I developed new techniques and explored material synthesis.

The contribution of Dr. Matthew Semler's experience and familiarity with all the lab equipment and instrumentation cannot be overstated. I also want to thank Drs. Sylvio

May, Warren Christensen, and Alan Denton for their advice and direction as I discerned research direction and career objectives. Sam Brown provided invaluable help on understanding solute chemistry and 3-D printing. Finally, I'd like to thank the MatBus drivers who provided much appreciated and timely transportation between my lab and S. Engineering.

DEDICATION

To Kristina and Isla, without whose unfathomable love and understanding

I would be a lesser man and no scientist at all.

TABLE OF CONTENTS

LIST OF FIGURES

LIST OF ABBREVIATIONS

AFM…….……..…….Atomic Force Microscopy

$AuCl_3$…….……..Gold Chloride

BOE…….……Buffered Oxide Etch

$(CH_3)_2CO$……..……..Acetone

CH_3NO_2……..…….Nitromethane

Cl…….……Chlorine

CoMoCat…….……Cobalt Molybdenum Catalyst

Cr……...…….…….Chromium

CNT……...……..Carbon Nanotube

CVD……...…….…….Carbon Vapor Deposition

EtOH……Ethanol

HF……Hydrofluoric Acid

Hg……... Mercury

K……..…….Kelvin

MHDS…….……. Hexamethyldisilazane

HP……..…..……Horsepower

MCE……...……..Mixed Cellulose Ester

mL…….…...……Milliliter

μL…….……Microliter

MPDIH20……...…..……Millipore-filtered deionized water

MWNT……..……..…….Multiwall Nanotube

NIST…….…..…….National Institute of Standards and Technology

nm……Nanometer

NSH…….……..……..Nanotube-Silicon Heterojunction

psi……Pounds per Square Inch

PDMS…….…… Polydimethylsiloxane

Si……...…..…….Silicon

SiO_2……..……..…..……Silicon Dioxide

$SOCl_2$……..Thionyl Chloride

SWNT……..…..…….….Single Wall Nanotube

SWCNT…….…….……Single Wall Carbon Nanotube

UV……...…….……Ultraviolet

vdW…….…….……..…….van der Waals

VFFS…….…….….Vacuum Flask Filtration System

1. INTRODUCTION

The search for stronger, lighter, cheaper, and more versatile materials is perennial in industry, academia and government. The fact that single-wall carbon nanotubes are orders of magnitude stronger and smaller than currently used building composites (1.2 TPa modulus, for example)[1] makes them of particular interest from a durability standpoint. Their conductivity and flexibility also recommend them for applications within the microelectronics industry.[2 3 4] Much as steel rebar strengthens a concrete structure, it has been suggested that nanotubes could be mixed into bulk materials to reinforce them. As somewhat limited success has been found with this approach, new ideas for exploiting both the structural and electrical properties of these materials are actively being sought. Because single-wall carbon nanotubes (SWCNTs) have dimensions on the order of a nanometer (nm), specialized ways to manipulate, bend, image, and measure their properties have to be utilized. Nanotubes conduct electricity as well as copper and can be implemented in novel field-effect transistor platforms and in solar-cell geometries as electrodes and emitters. Carbon nanotubes have a variety of applications, and herein we endeavor to characterize some of their useful structural properties.

In the realm of both structural and electronic applications, nanotube-loaded elastomers have been explored by the Department of Defense for their electromagnetic shielding properties, while nanotube films are being investigated by a number of research teams for applications in flexible electronics. At the other extreme, the dream of a space elevator lends itself to the high strength and low weight of carbon nanotubes. In aviation, defense, space science, and consumer electronics - as well as in academic and

government research - carbon nanotubes have solidified a place in future technology. The goal of the following research is to discover equipment and measurement methods for evaluating the bending and relaxing of single-wall carbon nanotube films in ethanol. It will involve the design and production of optical apparatuses, use of digital videography, and critiques of these methods and uses.

2. CARBON NANOTUBES

2.1. History

Carbon nanotubes are cylindrical allotropes of graphene with an aspect ratio of 100-100,000 and a diameter of approximately 1 nm.[5] Credit for the discovery of carbon nanotubes (CNT) is disputed between Soviet and Western scientists,[6] but single-walled carbon nanotubes (SWCNTs) were first shown in images by Morinobu Endo of the Centre National del la Recherche Scientifique.[7] Multi-walled carbon nanotubes (MWCNTs) consist of concentric SWCNTs, and have their own interesting production and implementation techniques. Both multi-walled and single-walled carbon nanotubes have been the subject of much interest and research in the physics, chemistry, and materials sciences communities in recent decades.

2.2. Production

One can imagine a nanotube as an sp^2 hybridized single-layer sheet of graphene rolled into an empty cylindrical straw.[8] As currently synthesized in large quantities, batches of nanotubes tend to contain 2/3 semiconducting and 1/3 metallic structures. The synthesis techniques used for the production of the nanotubes in our research are typically cobalt molybdenum catalyst (CoMoCat), laser-ablation, and arc-discharge.[9] [10] [11] A plasma torch method, which combines conditions of arc discharge and laser ablation, is also in use,[12] along with a Chemical Vapor Deposition (CVD) technique.[13] Generally, these schemes produce a carbon "soot" that clings to the chamber walls. This soot comprises a variety of structures, among which are SWCNTs.

2.3. Chirality

Nanotubes exist as metallic or semiconducting materials, the precise properties depending on the chirality of the nanotubes.[14 15 16] The honeycomb 2-dimensional lattice of graphene can be rolled to form a variety of tubular symmetries, which influence the electrical characteristics of the nanotube.[17 18 19] The chiral (*n*,*m*) vector, $\vec{C} = n\overrightarrow{a_1} + m\overrightarrow{a_2}$, characterizes the symmetry of this curling, and it determines whether the nanotube is semiconducting or metallic.[20] If $n - m$ is a multiple of 3, the nanotube is metallic.[21] Any other combination of n and m produces a semiconducting nanotube.[22]

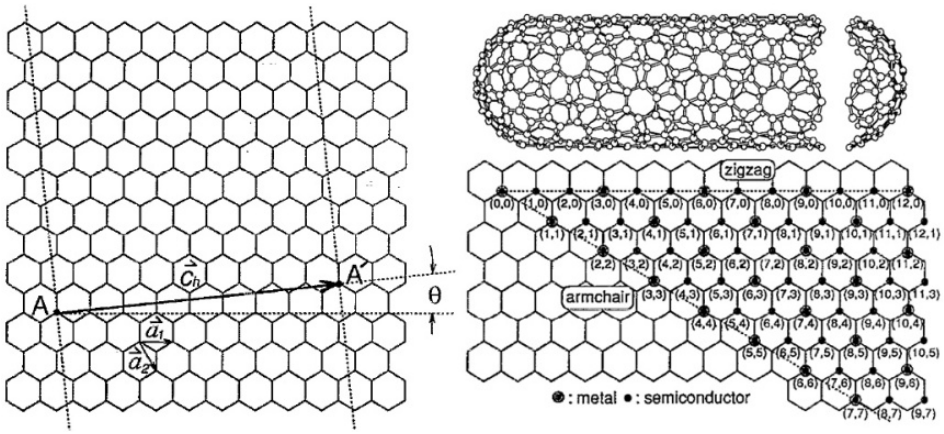

Figure 1: A chiral map indicating the various SWCNT geometries with metallic and semiconducting SWCNT structures. Zigzag and armchair nanotubes represent the symmetric boundary conditions for this map. The image is credited to the 1992 work of R. Saito *et al.*[23]

2.4. Sorting

The uniform sorting of SWCNTs by length, electronic type, and/or chirality has only recently been optimized to a point of sufficient efficiency.[24 25 26 27 28] The methods used by Yanagi et. al.[29] and Arnold et. al.[30] have been demonstrated to be effective, with additional degrees of sorting by the extent to which the tubes are filled with water.[31] Coarse centrifugation for 2 hours at 1885 rad/s in a Beckman-Coulter JA-20 rotor can be used to prepare a parent solution suitable for a number of courses, further separation or

forced filtration.[32] Specifically, such a mixed-type parent solution was used for film production and subsequent processing measurements detailed herein.

2.5. Bonding

SWCNTs interact with each other primarily *via* van der Waals (vdW) forces. These contacts can be described by anisotropic contact potential that depends on the radius and chirality of the nanotube and the angle at which contact is made.[33] [34] [35] Such vdW forces can be prodigious, so a surfactant is typically introduced to prevent premature bonding and agglomeration. The surfactant acts to fill in the gaps between nanotubes and allows them to slide by one another by surrounding the SCWNTs with a molecular layer, much as soap surrounds particulates of oil when one washes the dishes.

3. FILM PRODUCTION

3.1. Theory

While dispersing the nanotubes in a composite material has been investigated to a great extent,[36] the production of a nanoscale-thick SWCNT sheet with macroscopic lateral proportions comprised exclusively of single-wall nanotubes is of increasing academic and industrial interest.[37] [38] [39] Evidence shows that this method produces improvements over previous approaches, but it still fails to commend the microscopic moduli of a single nanotube to the sheet on a macroscopic scale. This makes the nanotube sheet approach a mere step toward the multifunctional materials that engineers and scientists ultimately seek to create. Nonetheless, such sheets are of considerable interest for a number of applications in flexible electronics.

3.2. Methodology

A collection of SWCNTs in a surfactant solution was provided by the National Institute of Standards and Technology (NIST) in unsorted, or polydisperse form. Mixed cellulose ester (MCE) filter paper was rinsed in Millipore-filtered deionized water (MPDIH20) to remove any dust particulates and then soaked in a 5 % solution of ethanol (EtOH) in MPDIH20. 200 mL of a 10 % solution of EtOH in MPDIH20 was prepared and manually degassed. To assemble the vacuum filtration system, a porous glass stage was fitted into a rubber bung in the opening of an Erlenmeyer flask with an evacuation port and leveled.

Figure 2: An image of the vacuum film filtration system (VFFS) used to produce the thin films of SWCNTs

The saturated filter paper was centered on the glass stage and a reservoir was attached with a clamp and then leveled. After adding the 10 % solution of EtOH to the reservoir while minimizing the introduction of bubbles, a GE Motors 5KCR38UN9292GX 1/3 HP pump was used to produce a 10 psi (20 inch Hg) reserve vacuum in a Napco Model 5831 Vacuum Oven. An FTS Systems SP Scientific VaporTrap was employed to condense water vapor, and the valve was eased open to begin drawing liquid from the reservoir into the vacuum flask.

Figure 3: The vacuum oven acted as a vacuum reservoir for the VFFS and to remove solvents from the finished film (left). The Vapor Trap kept gaseous water from entering the vacuum pump (right).

Using a 10 μL Eppendorf Reference volumetric pipette, nanotube solution was gently floated on the filter paper and allowed to settle as the EtOH solution was pulled through.

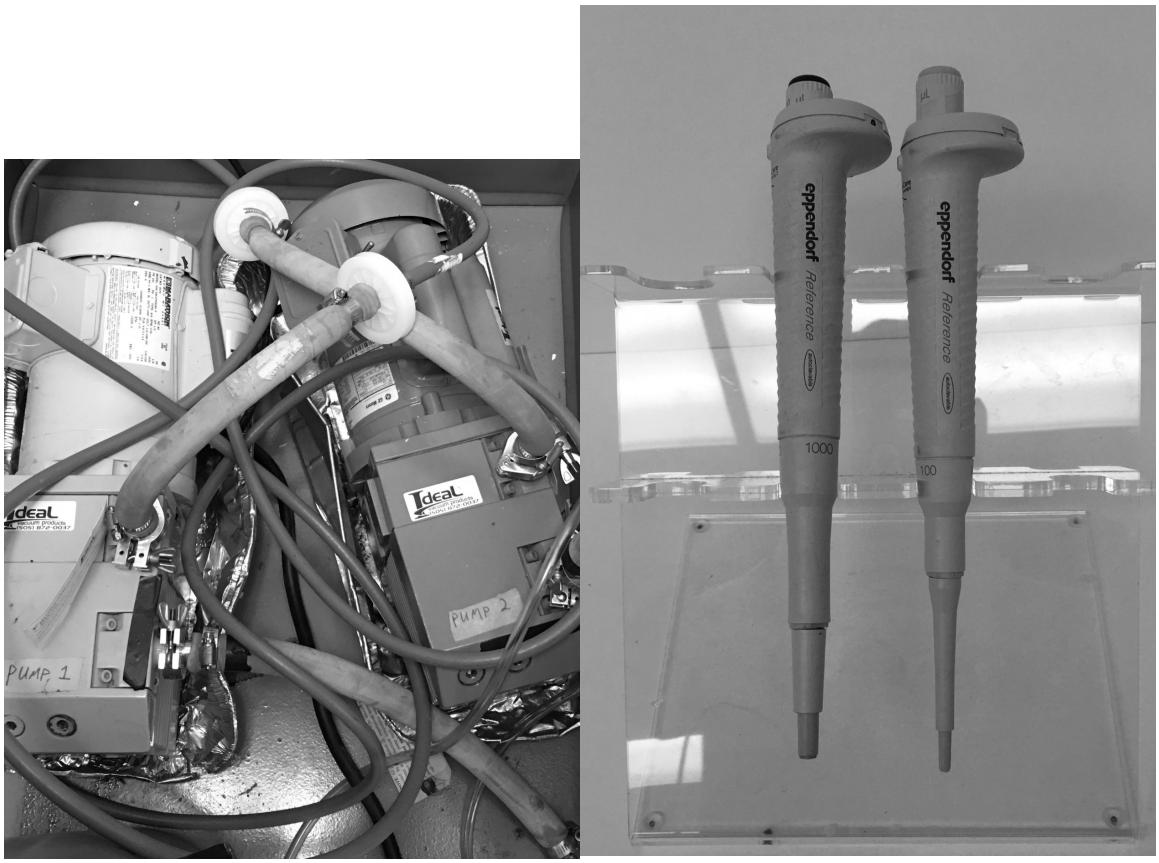

Figure 4: Vacuum Pumps (left). Volumetric Pipettes used to transfer nanofilms, Acetone, and Ethanol (right)

A volume of SWCNT solution was selected based on the intended thickness of the resultant film. Once the predetermined amount of SWCNTs were in place, the vacuum apparatus was allowed to run until the ethanol solution had been completely pulled through the filter. The result was a filter paper with a nanotube and surfactant film of uniform thickness. The perimeter of the filter paper was held flat as it was allowed to dry in a Napco Model 5831 Vacuum Oven. Film thicknesses varied from 10 to 200 nm as confirmed by atomic force microscopy (AFM) performed by John Harris.

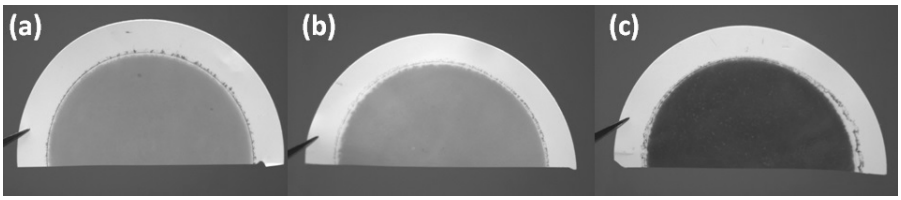

Figure 5: (a) Films of varied thickness and purity prepared on filter paper.

3.3. Surfactants and Solutions

The SWCNT film rests atop the MCE filter paper and must be separated before evaluation or application of the film can take place. Acetone, $(CH_3)_2CO$, was used to dissolve the MCE filter paper with minimal disturbance to the SWCNT film, although the precise nature of this interaction will be the topic of future research. To prevent SWCNT-SWCNT bonding in the parent solution, a surfactant was included in the liquid sample. Without removing the surfactant, the vdW interactions could not lead to the irreversible bonding of the SWCNTs necessary for film integrity. While acetone quickly and reliably dissolves the MCE, it also causes the filter paper to swell slightly. This effect occasionally resulted in the filter paper enlarging before it detached from the nanofilm, tearing the latter. While a method was tried of floating the film on the acetone so it could uniformly dissolve all parts of the filter paper at the same time, it provided limited improvement. Eventually, a method was devised wherein the film and filter paper were exposed to acetone vapors over the course of a few hours, allowing the sluggish swelling of the MCE before introduction by floating method in a shallow acetone bath. A series of baths was used with the film transferred to clean acetone each time in order to ensure maximum reduction of dissolved filter paper in and around the film.

Once the film was separated from the MCE, it still contained residual surfactant between the individual SWCNTs. An Eppendorf Reference volumetric pipette was used

to transfer the film from its acetone bath into a vial of absolute ethanol. The ethanol dissolved the remaining surfactant, leaving an integral film of SWCNTs bonded by vdW forces. Again, a series of baths was used to fully clean the surfactant from the nanofilm.

4. SOLAR CELLS

4.1. Theoretical Background

According to the American Census Bureau, the rate at which the world uses energy has increased exponentially. Approximately 80 % of the world's energy demands are currently being met with the burning of fossil fuels.[20] As developing countries become more industrialized, their energy consumption will add to an already daunting rate of electrical demand. Solar energy will be an integral part of meeting the power requirements of our advancing world, but the cost of silicon-based technologies continues to make the option prohibitive for many regions—even within the developed world. This cost is fueled by the high-temperature requirements of crystalizing silicon, (Si) 1100 K.[20] The use of SWCNTs as a component of such devices may significantly reduce the cost of solar energy because the process can be solution-based.

4.2. Production

Below is a summary of the production protocol, which provides motivation for why exploration of the processing of these thin films is desirable. SWCNT networks become *p*-doped under a number of different conditions.[40] For the work in question, our research was focused on the chlorine (Cl) anion in the doping protocol through a 3-part chemical process consisting of (1) washing the active area with 1 % HF to remove oxides and clean the junction, (2) chemical doping with thionyl chloride ($SOCl_2$), and (3) chemical doping via spin coating gold chloride ($AuCl_3$) freshly dissolved in nitromethane (CH_3NO_2).[20]

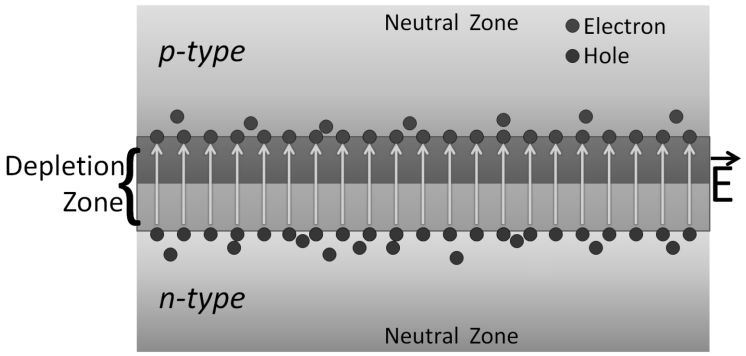

Figure 6: A P-N junction containing an electric field (yellow) as the result of charge separation in the heterojunction. In the standard forward-bias configuration, the *n*-type and *p*-type semiconductors are connected to the cathode and anode respectively.[20]

A SWCNT film was placed on a Silicon Dixode- (SiO_2) insulated electrode grid. The film dispersed in EtOH and positioned *via* bursts of air from a volumetric pipette. The goal was to cover the electrode fully without excess film margins outside the electrode.

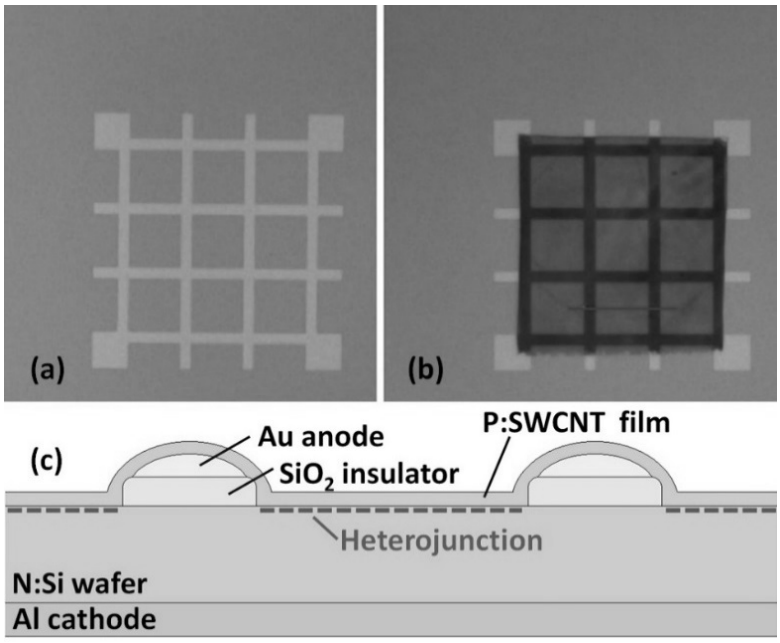

Figure 7: (a) A SiO_2-insulated electrode patterned into a grid with 1 mm spacing as described in chapter 3.1. (b) Supporting movies demonstrate the fluid mediated deposition process used to position a SWCNT film over the electrodes. (c) A cross section diagramming the device architecture across 2 electrodes indicated in (b) (not to scale).[20]

4.2.1. Masks and Film Application

After treating the wafer with hexamethyldisilazane (HMDS) to augment the adhesive properties between the wafer and the photoresist, a 1 μm photoresist layer was spin-coated on and baked for 1 minute at 373 K. The wafer being prepared was set below a clear-field Mylar shadow-mask and saturated with ultraviolet (UV) light for 13 seconds before another 1-minute bake at 373 K and bath in OPD 262 photodeveloper for 30 seconds, dissolving UV cross-linked photoresist. Remaining was a polymer cap on the dielectric of SiO_2. After curing at 393 K for 1 minute and submersion in buffered oxide etch (BOE), the crystalline silicon had transitioned from hydrophilic to hydrophobic, confirming the completion of the etching.

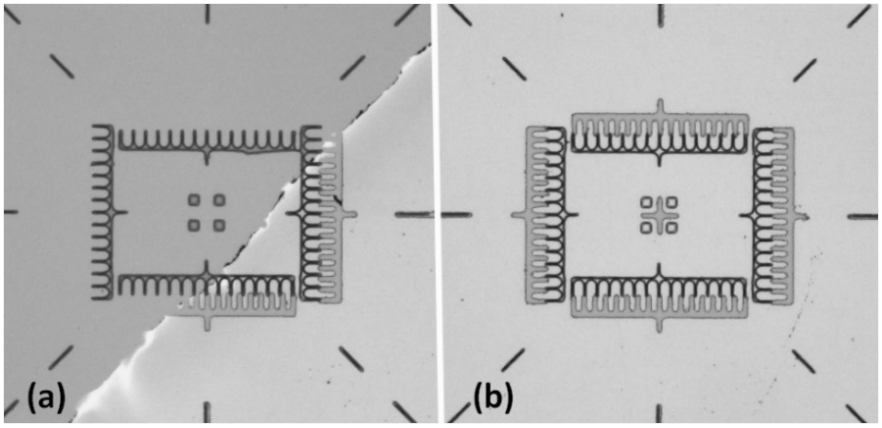

Figure 8: Dual Vernier comb alignment markers were used to accurately position the dark-field Mylar mask (outer-comb) over the patterned SiO_2 dielectric (inner-comb) in preparation for UV exposure. Kapton tape was used to mask (a) prior to Cr/Au/Cr deposition covering (b).[20]

4.2.2. Testing

Having been prepared on optical-grade quartz, the SWCNT films were measured for their electronic and optical properties.[41] [42] Film thickness, being an important component of the devices, was evaluated using a Digital Instruments Inc. Dimension 3100 atomic force microscope (AFM) operated in tapping mode.

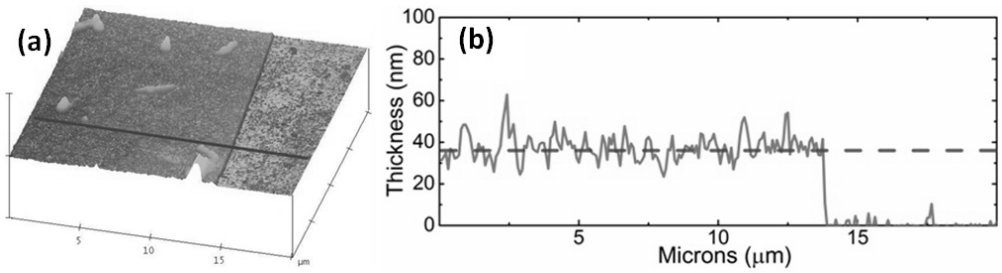

Figure 9: (a) Tapping mode AFM was used to scan SWCNT film edges at multiple points to yield film thickness through several cross-sectioned (b) step height measurements.[20]

A Photo Emission Tech Inc. SS50AAA solar simulator was used with a Keithley 2400 source meter and 2000 multimeter to give the IV profile. By using a PV Mesurements Inc. QE/ICPE QEX7 Measurements System, external quantum efficiency (EQE) was found. Temperature-dependent dark currents were measured by placing the NSH solar cell on a hot plate isolated from ambient light. At 20 K steps from 293 K to 393 K, Agilent probes gave the IV profile, which could be analyzed to yield ideality, Schottky barrier height, and the Richardson constant of the devices.

5. VIDEO SETUP

5.1. Theoretical Background

At the heart of experimental physics is measurability. Digital videography of the films' motion has the potential to allow us to examine the movement—bending and relaxing—of the films in a time-demarcated and processable manner. It would also allow us to transfer, back up, and compress the videos as necessary and prudent. Each pixel in each frame either represents the film or the background.

5.2. Equipment

A PL-B954HU digital video camera was used, collecting images at 16.6723 frames per second through a Tamron MVL75L Manual Focus and Manual Iris Fixed Focal Length Closed-Circuit Television telephoto lens.

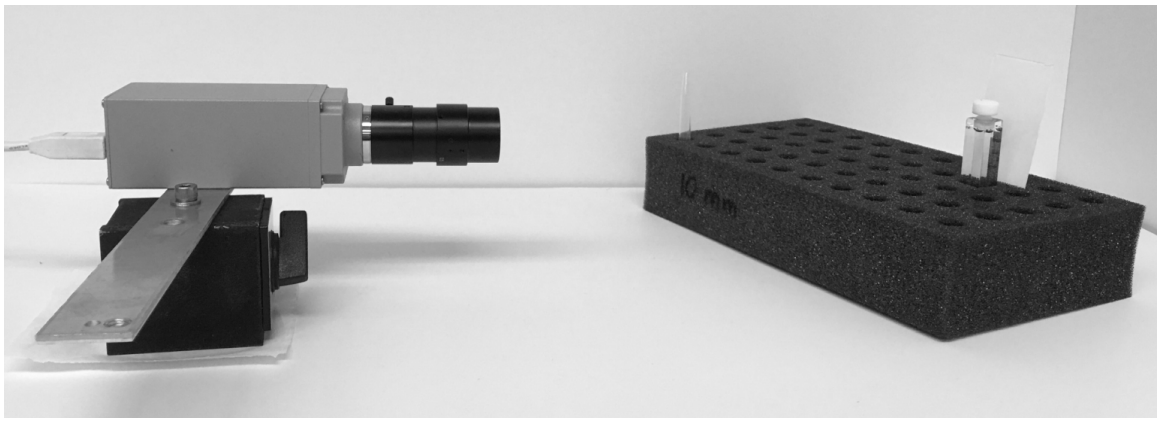

Figure 10: Example of Videographic Setup with Camera and Cuvette

Round borosilicate vials of 25 mL, 5 mL, and 2 mL, along with 100 mL, 200 mL and 500mL beakers were initially used for convenience, cost, and access. Eventually we began employing square-prism quartz cuvettes for their ease and optical superiority.

Figure 11: SWCNT Nanofilm suspended in EtOH within a Quartz Cuvette

5.3. Software

To interface the digital video camera with a computer and successfully capture the sequences of images, PixeLINK Release 7.25 Version 1.5.2.0 was utilized.. This offered a variety of options for exposure and frame rate. As the full-resolution uncompressed files produced by the PixeLINK software were often in excess of a gigabyte and contained more image data than we were interested in, the public domain program ImageJ 1.48v developed by Wayne Rasband of the National Institutes of Health was utilized to process the images. This program facilely enables the researcher to adjust a color video as individual frame images, isolate background from film of interest, and compress files without losing the data of interest.

5.4. Angles and Optical Aberration

Initially, experiments were set up to take place with the focus along the diameter of the round vials to minimize optical irregularities. Videos were taken from below (through the bottom of) the round glass containers later to give a flat and more uniform view of the thin films. Our round containers were not designed for optical use as we

were employing them, and when shooting from the side, the farther the pixels were from the diameter of the vials, the more optical aberration occurred. When videographing from the bottom, rings from the glass production introduced shadows and irregularities to the images.

5.5. Novel Approaches

Optical-grade square-prism quartz cuvettes were employed to minimize edge and end effects and provide the clearest and least distorted images. These like the other optical vessels were cleaned with Kim Wipes and 1-propenyl to remove dirt, dust, and oil. Without the aberration from curved and microcrystalline imperfections, less processing was required to analyze the movement of the films in ethanol.

6. FLOW HISTORY

6.1. Theoretical Background

In an attempt to better understand the film mechanics and potentially measure the Young's modulus of the parent nanofilms, we needed to repeatably and reliably deform them. While a number of different techniques were attempted, the work fell into two main categories: rotational method and constant flow. These techniques were expected to let us curl or wave the films as the ethanol fluid resisted their movement.

6.2. Experimental Procedures

The goal of flow history was to understand how the film moved within ethanol when it was spun around a central cylinder or caused to wave by a passing flow of ethanol. Once we had decided on the procedures to use, we had to design and fabricate the equipment in which to conduct the measurements.

6.2.1. Tank Production

Given the non-ideal optical nature of circular vessels for videography, a flat-sided vessel was sought. In an attempt to save the research group the cost of quartz cuvettes, A tank was fabricated out of microscope slides adhered at right angles to form a square prism with one open end.

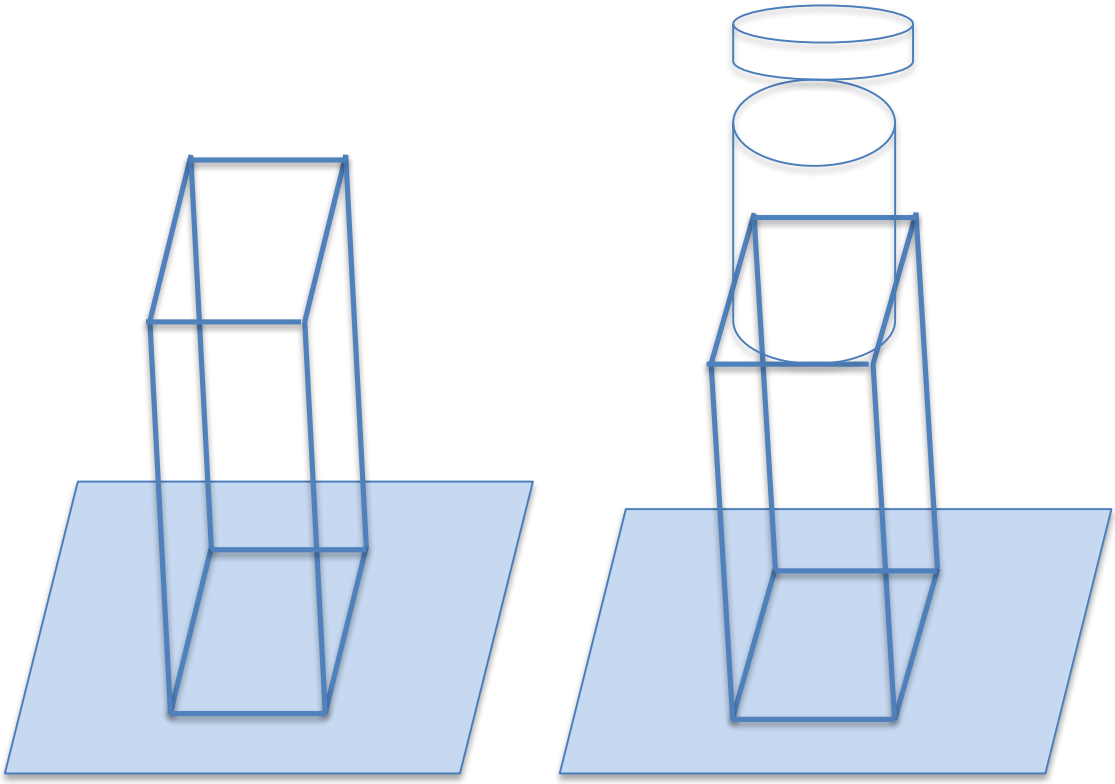

Figure 12: Experimental tank fabricated from microscope slides, open on top (left). Tank modified to allow sealing (right).

Four tanks were built, each on a 50 mm x 75 mm microscope slide: 50 mm x 50 mm x 75 mm, 37 mm x 37 mm x 75 mm, 25 mm x 25 mm x 75 mm, and 25 mm x 25 mm x 75 mm with an adapted sealable end. An epoxy compound was found that had low solubility in ethanol, and that was used at all joints.

6.2.2. Rotational Method

As the film is flexible, wrapping it around a spinning pole—much as a flag gets wrapped in a windstorm—seemed a viable option: the unfurling of the nanoflag could then potentially provide us with information about its mechanical properties.

Figure 13: A SWCNT Nanofilm furled around a central glass rod.

An LTA-HS rotational stage controlled by a Newport Motion Controller Model ESP301 was adapted to allow programmable, measured rotation of the pole about a central axis. A 1.6 mm x 100 mm hollow glass rod was used as the pole with the film—on filter paper—glued to the outer edge. It was found that this method provided unreliable adhesion, and the cement disturbed the flow of ethanol during spinning.

Dr. Matthew Semler used a laser to cut a slit through one side of the glass cylinder, allowing the adhesion of our film to the inside of the tube with polydimethylsiloxane (PDMS) at a 10:1 mixture.

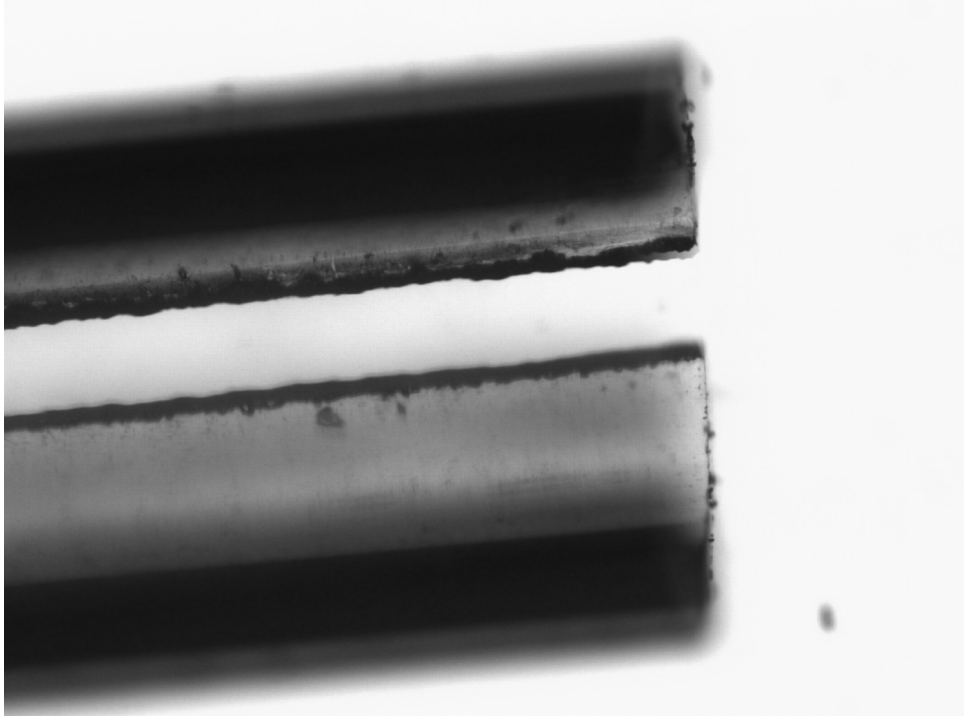

Figure 14: Optical Micrograph of a laser-etched glass micropipetting tube

Figure 15: A nanofilm on filter paper attached to the inside of a glass tube

The PDMS expanded when exposed to acetone, occasionally resulting in a tear of the nanofilm, so a 2-part epoxy was utilized. Even so, the serrated nature of the laser-cut edges cut the films if spun too fast. The use of a butane torch to melt and smooth the edges proved useful, albeit cumbersome. The problem remained that the nanoflag was denser than the surrounding EtOH, leading it to droop and exert uneven strain on the interface with the central glass rod.

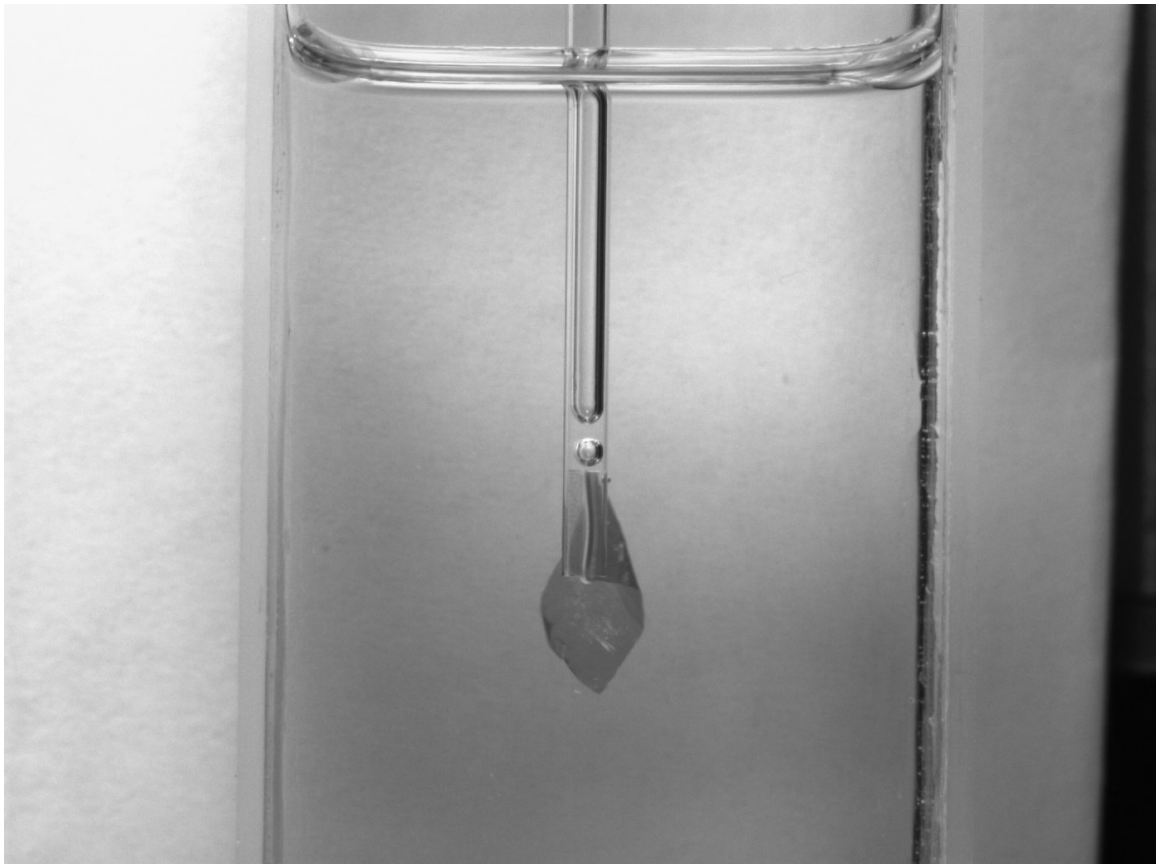

Figure 16: Drooping nanoflag connected to central rod.

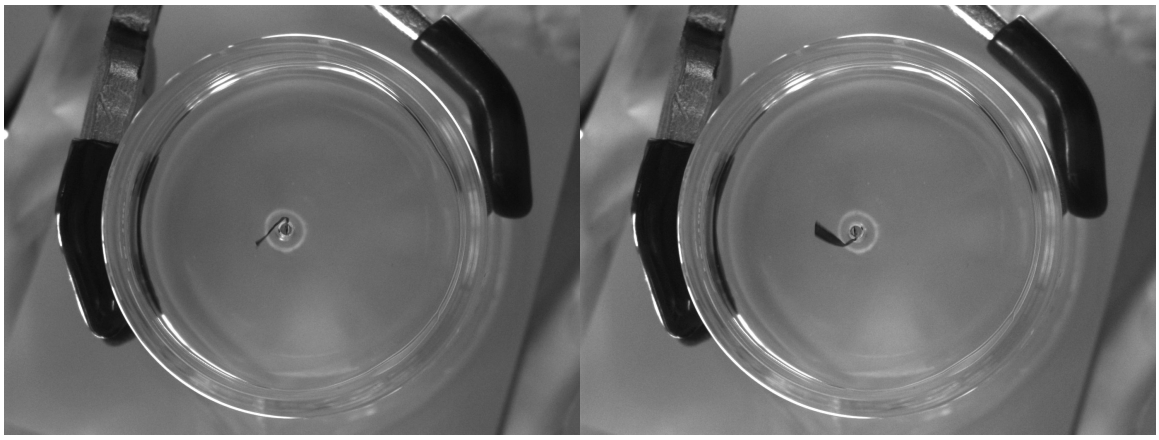

Figure 17: Nanoflag with sharp crease at interface with rod (left). Nanoflag unfurling (right)

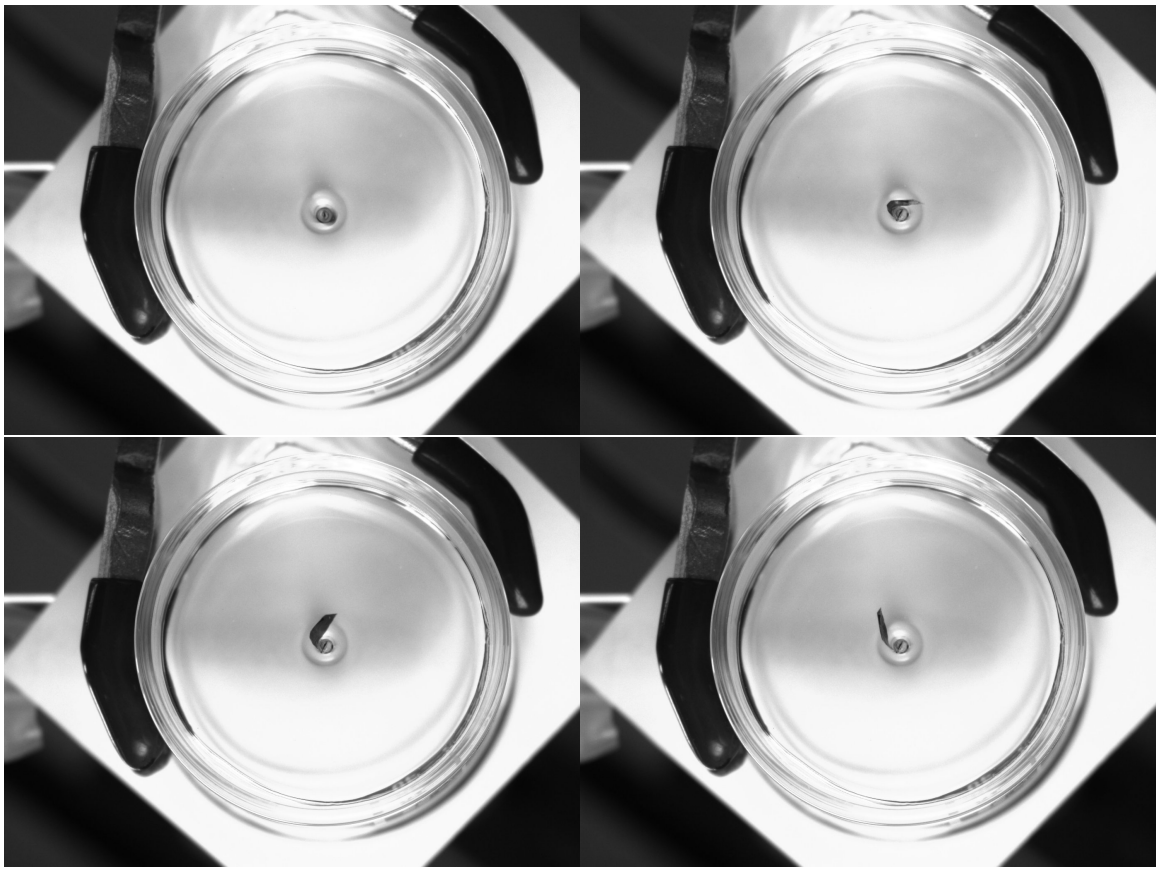

Figure 18: A Nanoflag completely wrapped (top-left). Nanoflag as it unfurls (remaining).

6.2.3. Constant Flow

Given the problematic nature of spinning and unfurling the nanoflag, a different approach was pursued. Both the process of waving the flag orthogonal to its face and an

attempt of passing fluid past the film—akin to a flag in constant wind—were made. Here, an LTA-HS rotational stage controlled by a Newport Motion Controller Model ESP301 was applied as designed to wave the flag, sandwiched between two pieces of polished crystallized silicon wafer.

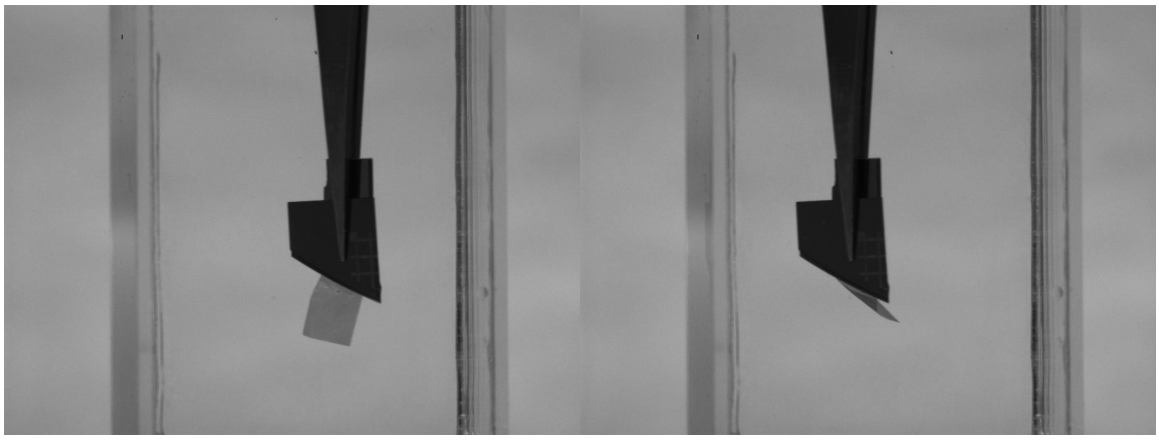

Figure 19: Nanoflag sandwiched between silicon wafer fragments (left). Nanoflag waving as EtOH resists its motion (right).

A flow chamber was 3-D printed out of plastic by Sam Brown that would allow the constant flow of ethanol, the insertion of the "flag pole," and the videography through a glass side. Before the assembly of the pumps was complete, a new direction had been decided on, making the constant flow experiment unnecessary. It was realized that the impact of film rigidity on the motion of the flag was of too high an order to provide precise insight. This understood by simply referring back to an actual flag; in a strong wind (i.e., strong flow), a cloth flag appears rigid, despite in fact being soft.

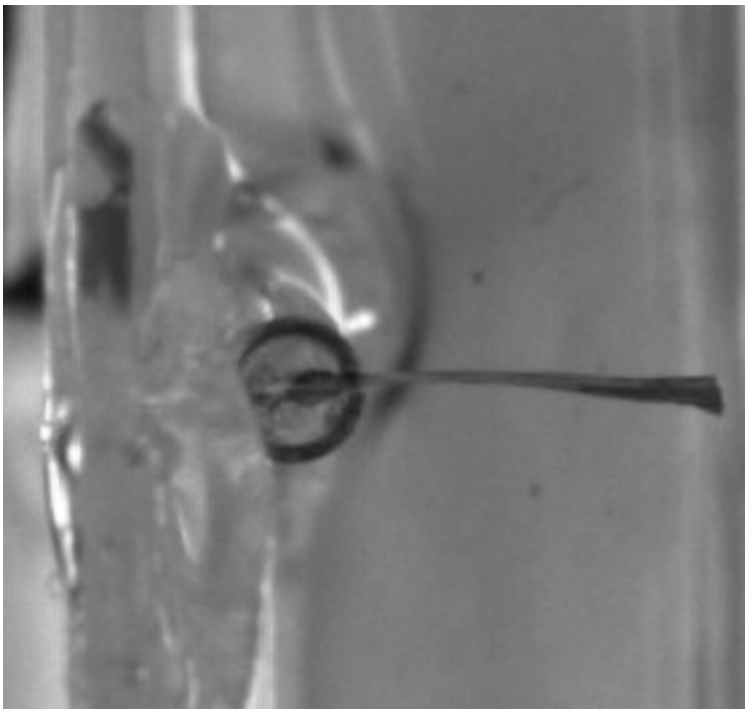

Figure 20: A Nanoflag in flow chamber

Although many new ideas along these lines were investigated, these are not included in this document because they are proprietary to NDSU. This additional work was, however, included in my thesis defense and is privy to the thesis committee. The groundwork outlined here served as a basis for the further mechanical characterization SWCNT films, which will be reported in a future publication.

7. CONCLUSIONS

As is often the case in scientific research, a number of methods were found that failed to provide complete and successful results. Optical aberration was a significant shortcoming of the initial experimental setup, as was the modeling of flow. Mechanically manipulating any portion of the flag tended to destroy the nanofilm. Future work will focus on new methods to manipulate the SWCNT film using magnetic, rather than mechanical means.

REFERENCES

[1] R. Saito, G. Dresselhaus, M. S. Dresselhaus, Physical Properties of Carbon Nanotubes (Imperial College Press, 1999).

[2] R. H. Baughman, A. A. Zakhidov, W. A. de Heer, "Carbon nanotubes - the route toward applications", Science 297, 787-792 (2002).

[3] Z. Wu, Z. Chen, X. Du, J. M. Logan, J. Sippel, M. Nikolou, K. Kamaras, J. R. Reynolds, D. B. Tanner, A. F. Hebard, A. G. Rinzler, "Transparent, conductive carbon nanotube films", Science 305, 1273 (2004).

[4] Q. Cao, J. A. Rogers, "Ultrathin films of single-walled carbon nanotubes for electronics and sensors: A review of fundamental and applied aspects", Adv. Mater. 21, 29-53 (2008).

[5] R. Saito, G. Dresselhaus, M. S. Dresselhaus, Physical Properties of Carbon Nanotubes (Imperial College Press, 1999).

[6] Pacios Pujadó, Mercè (2012). *Carbon Nanotubes as Platforms for Biosensors with Electrochemical and Electronic Transduction*. Springer Heidelberg. pp. XX,208.

[7] Pacios Pujadó, Mercè (2012). *Carbon Nanotubes as Platforms for Biosensors with Electrochemical and Electronic Transduction*. Springer Heidelberg. pp. XX,208.

[8] John Michael Harris, "The Nature of Single-Wall Carbon Nanotube Silicon Heterojunction Solar Cells", A Dissertation Submitted to the Graduate Faculty of North Dakota State University of Agricultural and Applied Science. 9 (2015)

[9] Scott, C.D., Arepalli, S., Nikolaev, P., Smalley, R.E. "Growth Mechanisms for Single Wall Carbon Nanotubes in a Laser-Ablation Process" J Appl. Phys. A, 72,574-580, (2001).

[10] Shi, Z., Lian, Y., Liao, F. H., Zhou, X., Gu, Z., Zhang, Y., Iijima S., Li, H., Yue, K.T., Zhang, S.L; "Large Scale Synthesis of Single-Wall Carbon Nanotubes by Arc-Discharge Method" J. Phys. Chem. Solids, 61, 1031-1036, (2000).

[11] Resasco, D.E., Alvarez, W.E., Pompeo, F., Balzano, L., Herrera, J.E., Kitiyanan, B. and Borgna, A., "A Scalable Process for Production of Single-Walled Carbon Nanotubes by Catalytic Disproportionation of CO on a Solid Catalyst" J. Nanopart. Res., 4, 131-136, (2002).

[12] Smiljanic, Olivier; Stansfield, B.L.; Dodelet, J.-P.; Serventi, A.; Désilets, S. (22 April 2002). "Gas-phase synthesis of SWNT by an atmospheric pressure plasma jet". *Chemical Physics Letters* 356 (3–4): 189–193.

[13] Beckman, Wendy (2007-04-27). "UC Researchers Shatter World Records with Length of Carbon Nanotube Arrays". University of Cincinnati.

[14] R. Saito, G. Dresselhaus, M. S. Dresselhaus, Physical Properties of Carbon Nanotubes (Imperial College Press, 1999).

[15] M. S. Arnold, A. A. Green, J. F. Hulvat, S. I. Stupp, M. C. Hersam, “Sorting carbon nanotubes by electronic structure using density differentiation”, Nature Nanotechnology 1, 60-65 (2006).

[16] K. Yanagi, Y. Miyata, H. Kataura, “Optical and conductive characteristics of metallic single-wall carbon nanotubes with three basic colors; Cyan, magenta, and yellow”, Appl. Phys. Express 1, 034003 (2008).

[17] R. Saito, G. Dresselhaus, M. S. Dresselhaus, Physical Properties of Carbon Nanotubes (Imperial College Press, 1999).

[18] M. S. Arnold, A. A. Green, J. F. Hulvat, S. I. Stupp, M. C. Hersam, “Sorting

carbon nanotubes by electronic structure using density differentiation", Nature Nanotechnology 1, 60-65 (2006).

[19] K. Yanagi, Y. Miyata, H. Kataura, "Optical and conductive characteristics of metallic single-wall carbon nanotubes with three basic colors; Cyan, magenta, and yellow", Appl. Phys. Express 1, 034003 (2008).

[20] John Michael Harris, "The Nature of Single-Wall Carbon Nanotube Silicon Heterojunction Solar Cells", A Dissertation Submitted to the Graduate Faculty of North Dakota State University of Agricultural and Applied Science. 9 (2015)

[21] Saito, R.., Fujita, M., Dresselhaus, G., and Dresselhaus, M.S., "Electronic Structure of Chiral Graphene Tubules", Appl. Phys. Lett., 60, 2204-2206, (1992).

[22] Saito, R.., Fujita, M., Dresselhaus, G., and Dresselhaus, M.S., "Electronic Structure of Chiral Graphene Tubules", Appl. Phys. Lett., 60, 2204-2206, (1992).

[23] Saito, R.., Fujita, M., Dresselhaus, G., and Dresselhaus, M.S., "Electronic Structure of Chiral Graphene Tubules", Appl. Phys. Lett., 60, 2204-2206, (1992).

[24] Yanagi, K., Miyata, Y., and Kataura, H., "Optical and Conductive Characteristics of Metallic Single-Wall Carbon Nanotubes with Three Basic Colors; Cyan, Magenta, and Yellow", Appl. Phys. Express, 1, 034003, (2008).

[25] Fagan, J. A., Becker, M. L., Chun, J., and Hobbie, E. K., "Length Fractionation of Carbon Nanotubes Using Centrifugation", Adv. Mater., 20, 1609-1613, (2008).

[26] Arnold, M. S., Suntivich, J., Stupp, S. I., and Hersam, M. C., "Hydrodynamic Characterization of Surfactant Encapsulated Carbon Nanotubes Using an Analytical Ultracentrifuge", ACS Nano, 2, 2291-2300, (2008).

[27] Tu, X., Manohar, S., Jagota, A., and Zheng, M., "DNA Sequence Motifs for Structure

Specific Recognition and Separation of Carbon Nanotubes," Nature, 460, 250-253, (2009).

[28] Fagan, J. A., Becker, M. L., Chun, J., Nie, P., Bauer, B. J., Simpson, J. R., Hight-Walker, A., and Hobbie, E. K., "Centrifugal length separation of carbon nanotubes", Langmuir, 24, 13880-13889, (2008).

[29] Yanagi, K.., Miyata, Y., and Kataura, H., "Optical and Conductive Characteristics of Metallic Single-Wall Carbon Nanotubes with Three Basic Colors; Cyan, Magenta, and Yellow", Applied Physics Express, 1, 034003, (2008).

[30] Arnold, M. S., Green, A. A., Hulvat, J. F., Stupp, S. I., and Hersam, M. C., "Sorting carbon nanotubes by electronic structure using density differentiation", Nature Nanotech., 1, 60-65, (2006).

[31] Fagan, J. A., Huh, J.-Y., Simpson, J. R., Blackburn, J. L., Holt, J. M., Larsen, B. A., and Hight Walker, A. R., "Separation of Empty and Water-Filled Single-Wall Carbon Nanotubes", ACS Nano, 5, 3943-3953, (2011).

[32] Fagan, J. A., Becker, M. L., Chun, J., Nie, P., Bauer, B. J., Simpson, J. R., Hight Walker, A. R. and Hobbie, E. K., "Centrifugal Length Separation of Carbon Nanotubes", Langmuir, 24, 13880-13889, (2008).

[33] I. Ostanin, R. Ballarini, D. Potyondy, T. Dumitrică, "A distinct element method for large scale simulations of carbon nanotube assemblies", J. Mech. Phys. Solids 61, 762-782 (2013).

[34] T. Anderson, E. Akatyeva, I. Nikiforov, D. Potyondy, R. Ballarini, T. Dumitrică, "Toward distinct element method simulations of carbon nanotube systems", ASME J. Nanotech. Eng. and Med. 1, 041009-5 (2010).

[35] MEP/Collaborative Research: A New Paradigm for Hybrid Carbon Nanotube Composites, 5

[36] Q. Li, M. Zaiser, J. R. Blackford, C. Jeffree, Y. He, V. Koutsos, "Mechanical properties and microstructure of single-wall carbon nanotube/elastomeric epoxy composites with block copolymers", Mater. Lett. 125, 116-119 (2014).

[37] J. Zhu, W. Cao, M. Yue, Y. Hou, J. Han, M. Yang, "Strong and stiff aramid nanofiber/carbon nanotube nanocomposites", ACS Nano 9, 2489-2501 (2015).

[38] J.-W. Kim, E. J. Siochi, J. Carpena-Núñez, K. E. Wise, J. W. Connell, Y. Lin, R. A. Wincheski, "Polyaniline/carbon nanotube sheet nanocomposites: Fabrication and characterization", ACS Appl. Mater. & Interfaces 5, 8597-8606 (2013).

[39] J.-W. Kim, G. Sauti, E. J. Siochi, J. G. Smith, R. A. Wincheski, R. J. Cano, J. W. Connell, K. E. Wise, "Toward high performance thermoset/carbon nanotube sheet nanocomposites via resistive heating assisted infiltration and cure", ACS Appl. Mater. Interfaces 6, 18832-18843 (2014).

[40] Harris, J. M., Iyer, S.G.R., Hobbie E.K., Bernhardt, A.K., Huh J.Y., Hudson S.D., and Fagan J.A., "Electronic Durability of Flexible Transparent Films from Type-Specific Single-Wall Carbon Nanotubes" ACS Nano, 6,881-887, (2012).

[41] Harris, J. M., Huh, J. Y., Semler, M. R., Ihle, T., Stafford, C. M., Hudson, S. D., Fagan, J. A., and Hobbie, E. K., "Elasticity and Rigidity Percolation in Flexible Carbon Nanotube Films on PDMS Substrates" Soft Matter, 9, 11568-11575 (2013).